Spectroscopic Studies of Photosystem II in Chlorophyll *d*-Containing *Acaryochloris marina*[†]

M. Reza Razeghifard,*[,‡] Min Chen,[‡] Joseph L. Hughes,[§] Joel Freeman,[‡] Elmars Krausz,[§] and Tom Wydrzynski[‡]

Photobioenergetics, Research School of Biological Sciences and Research School of Chemistry, The Australian National University, Canberra, ACT 0200, Australia

Received August 6, 2004; Revised Manuscript Received June 23, 2005

ABSTRACT: Photosystem II (PSII) electron transfer (ET) in the chlorophyll *d*-containing cyanobacterium *Acaryochloris marina* (*A. marina*) was studied by time-resolved electron paramagnetic resonance (EPR) spectroscopy at room temperature, chlorophyll fluorescence, and low-temperature optical spectroscopy. To maximize the ability to measure PSII ET in the intact cells of this organism, growth conditions were optimized to provide the highest specific O_2 activity and the instrumental parameters for the EPR measurements of tyrosine Z (Y_Z) reduction were adjusted to give the best signal-to-noise over spectral resolution. Analysis of the $Y_Z^{\bullet}$ reduction kinetics revealed that ET to the oxygen-evolving complex on the donor side of PSII in *A. marina* is indistinguishable from that in higher plants and other cyanobacteria. Likewise, the charge recombination kinetics between the first plastoquinone acceptor Q_A and the donor side of PSII monitored by the chlorophyll fluorescence decay on the seconds time scale are not significantly different between *A. marina* and non-chlorophyll *d* organisms, while low-temperature optical absorption spectroscopy identified the primary electron acceptor in *A. marina* as pheophytin *a*. The results indicate that, if the PSII primary electron donor in *A. marina* is made up of chlorophyll *d* instead of chlorophyll *a*, then there must be very different interactions with the protein environment to account for the ET properties, which are similar to higher plants and other cyanobacteria. Nevertheless, the water oxidation mechanism in *A. marina* is kinetically unaltered.

The light reactions in oxygenic photosynthesis are catalyzed by photosystem I (PSI) and photosystem II (PSII),[1] which are embedded in the thylakoid membranes of plants, algae, and cyanobacteria. PSII is directly responsible for the photo-oxidation of water, ultimately providing electrons for PSI and releasing O_2 as a byproduct. PSI catalyzes the formation of the strong reductant NADPH that is used in the Calvin−Benson−Bassham cycle for the assimilation of carbon into organic compounds. During the light reactions in oxygenic photosynthesis, ATP is also produced from the proton gradients that are generated by electron transfer (ET). Both PSII and PSI are multisubunit, pigment−protein complexes that incorporate chlorophyll (Chl) molecules into light harvesting as well as photochemical components to convert light energy into oxidation potential and electron flow. Electrons are initially generated by the photo-oxidation of a special reaction center Chl complex called the primary electron donor. Even though the reaction centers in all photosynthetic organisms share the same basic principles in carrying out photochemical events, PSII is unique in that it provides the necessary oxidation potential to drive the oxidation of water. In anoxygenic photosynthetic bacteria, for example, only one photosystem containing bacteriochlorophyll (BChl) is used in a cyclic ET pathway to generate ATP. On the other hand, both PSII and PSI are required to work in tandem in a noncyclic ET pathway to generate the more energy-rich intermediates of oxygenic photosynthesis. Nonetheless, the organization of the PSII reaction center shows astonishing similarities to that of the photosynthetic purple bacteria, particularly on the acceptor side, suggesting that the reaction centers are evolutionarily linked (*1*). However, one important difference is that in PSII the Chl *a*, which absorbs at shorter wavelengths of light than the BChl *a*, provides the higher energy needed for the oxidation of water into molecular oxygen (which has a midpoint potential of +870 mV at pH 6). It is of particular interest, therefore, to study organisms such as *A. marina* that performs oxygenic photosynthesis but contains predominantly Chl *d* (*2*), which lies energetically between BChl *a* and Chl *a* (*3*).

Despite its unusual pigment composition, *A. marina* appears to have diverged within the cyanobacterial radiation (*4*) and is similar to Chl *a*-type cyanobacteria in that it contains two photosystems and carries out oxygenic photosynthesis. *A. marina* grows photoautotrophically in associa-

[†] This work was supported in part by a Human Frontier Science Program Grant (RGP0029/2002) and an Australian Research Council Discovery Grant (DP0450421).

* To whom correspondence should be addressed. Telephone: +61-(02)-61253980. Fax: +61-(02)-61258056. E-mail: reza.razeghifard@anu.edu.au.

[‡] Research School of Biological Sciences.

[§] Research School of Chemistry.

[1] Abbreviations: (B)Chl, (bacterio)chlorophyll; DCMU; 3-(3,4-dichlorophenyl)-1,1-dimethylurea; DMBQ; 2,3-dimethoxy-5-methyl-1,4-benzoquinone; EPR, electron paramagnetic resonance; ET, electron transfer; HEPES, *N*-2-hydroxyethyl piperazine-*N*′-*2*-ethanesulfonic acid; MES, 2-(*N*-morpholino)ethanesulfonic acid; MCD, magnetic circular dichroism; OEC, oxygen-evolving complex; PBQ, *p*-benzoquinone; Pheo, pheophytin; PSII, photosystem II; Y_Z, redox-active tyrosine of the D1 polypeptide; Y_D, redox-active tyrosine of the D2 polypeptide.

10.1021/bi048314c CCC: $30.25
Published on Web 00/00/0000 PAGE EST: 9.3

tion with a colonial ascidian together with Chl *a*/*b*-containing *Prochloron didemni* (*P. didemni*). Chl *a* is also found in *A. marina* but only as a minor component that appears to be localized mostly in PSII. The ratio of Chl *a*/Chl *d* varies between 0.03 and 0.1 depending on the growth conditions (*5*). The chemical structure of Chl *d* is different from Chl *a* in which the vinyl group on ring IV is replaced by a 3-formyl group. This structural difference results in a red shift by about 32 nm in the Q_y absorption band for Chl *d* in organic solvents compared with Chl *a*. In *A. marina* cells, the absorption maximum occurs at about 714−718 nm (*2*). The action spectra of both PSII and PSI complexes indicate that Chl *d* constitutes their antenna systems (*6*). *A. marina* seems to benefit from the use of Chl *d* by absorbing in the far-red light region (700−750 nm) that is not used by its companion cyanobacterium *P. didemni*, which contains only Chl *a* and Chl *b*. Until the discovery of *A. marina*, it was believed that all primary electron donors in oxygenic photosynthesis were invariably Chl *a* molecules. However, it has now been shown that the reaction center of PSI in *A. marina* uses a special pair of Chl *d*, which is called P_{740}, named after its flash-induced absorbance change maximum at 740 nm, as the primary electron donor (*7*).

Through the biophysical and biochemical characterization of isolated PSI samples, it became clear that the P_{740} dimer contains Chl *d* or Chl *d*′ (the epimer of Chl *d* at the 13^2 carbon in ring) (*7*, *8*) and has a midpoint potential (E_m) of +335 mV for P_{740}/P_{740}^+ (*7*). This midpoint potential is significantly lower than that of P_{700}/P_{700}^+ in other cyanobacteria, which has a value of about +450 to +480 mV (*9*, *10*); however, the reducing power of P_{740}^* seems to be equivalent to that of P_{700}^* (*7*). In contrast to the PSI reaction center, a clear determination of the chemical identity of the primary electron donor of PSII in *A. marina* has not yet been achieved. This uncertainty is mainly due to the difficulties associated with preparing highly purified, active PSII samples and/or with obtaining meaningful PSII signals in intact cells (in the presence of PSI) that are needed to determine PSII photochemistry and pigment composition. In general, the oxidized primary donor of PSI has a long lifetime extending to the millisecond range, while the oxidized primary donor of PSII is fully reduced within the microsecond time range. This kinetic difference makes the detection of the primary donor of PSII more difficult. On the basis of time-resolved fluorescence studies in the picosecond time range, it has been suggested that the primary electron donor of PSII in *A. marina* is composed of Chl *a* molecules (*11*); however, other reports propose that Chl *d* makes up the PSII primary electron donor (*12*, *13*).

The PSII core complex that contains the reaction center is composed of the D1, D2, and cyt b_{559} protein subunits. When the primary electron donor of PSII is photoexcited, it transfers an electron to the D1-bound pheophytin (Pheo) molecule in a few picoseconds, forming a radical pair. The charge separation is stabilized by the subsequent rapid transfer of the electron to a tightly bound plastoquinone molecule, Q_A, and then to a mobile plastoquinone molecule, Q_B. For all known Chl *a*-type PSII reaction centers, the oxidized primary electron donor ($P_{680}^{+\cdot}$) overcomes the energy barrier to oxidize water, which takes place at a manganese-containing catalytic site (i.e., the Mn_4Ca cluster). Four oxidizing equivalents are sequentially stored by increasing the redox state of the Mn_4Ca cluster. The sequential accumulation of four oxidizing equivalents was first observed in the period-four oscillations in the O_2 evolved from dark-adapted samples illuminated by short single-turnover flashes (*14*, *15*). This behavior is described by the S cycle in which the redox states of the Mn_4Ca cluster are labeled S_0-S_4. The index for each S state represents the number of oxidizing equivalents stored. O_2 is released as a result of spontaneous reduction of the S_4 state to the S_0 state.

On the donor side of PSII, the tyrosine residue at position 161 on the D1 polypeptide (*Synechocystis* numbering), Y_Z, acts as an intermediate electron carrier in transferring the oxidizing equivalents from the oxidized primary electron donor to the Mn_4Ca cluster (*16*, *17*). The oxidized Y_Z, which is deprotonated to the neutral radical ($Y_Z^{\cdot}$), is reduced by the Mn_4Ca cluster when advancing the S cycle from the S_n to the S_{n+1} state. The oxidized Y_Z is a paramagnetic species and gives rise to a transient EPR signal in intact systems (*18*, *19*). Thus, the rate of S-state transitions can be obtained by measuring the $Y_Z^{\cdot}$ rereduction rate using EPR.

There is another spectroscopically similar EPR signal that originates from the tyrosine residue at position 161 on the D2 polypeptide, Y_D, upon oxidation. However, Y_D is not directly involved in the water oxidation chemistry (*16*, *20*). Unlike $Y_Z^{\cdot}$, the $Y_D^{\cdot}$ signal is very long-lived in the dark (*21*). The S-state transition rates are indicators for the intactness of the water-oxidizing enzyme and are slowed in PSII membrane preparations and when PSII centers are genetically modified (*22*, *23*). The rates are also affected when the reaction conditions are moved away from optimal, such as by changing pH, thus providing some mechanistic insights into the enzyme function (*24*).

On the acceptor side, the photoactive Pheo can be identified by a large electrochromic shift induced in the Q_x transition of this pigment near 550 nm. This effect was originally noted as the C550 shift in transient optical experiments at room temperature (*25*−*27*). However, the $S_1(Q_A^-)$ state is very long-lived at low temperatures, and the electrochromic shifts and spectral locations for both Q_x and Q_y of the photoactive Pheo can be determined by appropriate illumination of PSII samples and precision absorption measurements in both the S_1 and $S_1(Q_A^-)$ states (*28*).

In this work, we have studied the properties of the primary electron donor of PSII in *A. marina* by measuring the ET rates on the donor side and monitoring the charge recombination with the acceptor side using time-resolved EPR and fluorescence techniques, respectively. The ET rates at room temperature were used to determine the oxidation efficiency of the primary electron donor in *A. marina* in comparison with the $P_{680}^{+\cdot}$ in *Synechocystis* PCC 6803 (*S.* 6803) as the control. The spectral characterization of the photoactive Pheo was achieved by low-temperature illumination spectroscopy. Growth conditions and technical parameters were improved to optimize the experimental conditions for obtaining unambiguous signals from intact cells.

MATERIALS AND METHODS

Spinach Thylakoids. Thylakoid membranes were isolated from market spinach leaves in dim light. About 100 g of

leaves were deveined and homogenized in 50 mM *N*-2-hydroxyethyl piperazine-*N*′-*2*-ethanesulfonic acid (HEPES)−NaOH (pH 7.5), 50 mM NaCl, 5 mM $MgCl_2$, and 0.4 M sucrose. The homogenate was filtered through eight layers of cheesecloth and one layer of nylon mesh before centrifugation at 1000*g* for 10 min. The pellet was resuspended in 100 mL of 50 mM HEPES−NaOH (pH 7.5), 50 mM NaCl, and 5 mM $MgCl_2$ to give an osmotic shock and then centrifuged at 1000*g* for 10 min. The pellet of thylakoid membranes was finally resuspended in homogenizing buffer at 1.5 mg of Chl/mL. The O_2 evolution of thylakoids was between 220 and 250 μmol of O_2 (mg of Chl)$^{-1}$ h^{-1} in the presence of 2 mM NH_4Cl as uncoupler and artificial electron acceptors [0.25 mM 2,3-dimethoxy-5-methyl-1,4-benzoquinone (DMBQ) and 0.25 mM $K_3Fe(CN)_6$]. Chl concentrations were determined in 80% acetone by the method of Porra et al. (*29*).

Cyanobacterial Samples. Cells in 16-L batches were grown photoautotrophically under axenic conditions with continuous aeration at 28 °C. Metal-arc lamps (General Electric 1000 W multivapor, metal−halide lamps) were used as the light source with the light intensity adjusted to 60 μmol of photons m^{-2} s^{-1}. *A. marina* was grown in ESS medium, which contained ES additives in seawater as previously described (*30*). The O_2 activity of the culture was monitored daily to determine the optimal time for harvesting the cells. Under our experimental conditions, the optimal time was 5 days after incubation. For cultures older than 5 days, the O_2 activity would drop even though the cells remained viable. *S.* 6803 was grown in BG-11 medium supplemented with 5 mM TES−NaOH (pH 8.0) and 5 mM sterile-filtered glucose (*31*). Cells were harvested by centrifugation at 3000 rpm for 10 min in a Sorvall GS3 rotor. Chl was extracted in 100% methanol, and the concentration was estimated using the extinction coefficient (mg/mL) 79.24 at 665.2 nm and 110.2 at 696 nm for *S.* 6803 and *A. marina*, respectively. Thylakoid membranes of *A. marina* were isolated from freshly harvested cells as described previously (*31*). Cells suspended in 50 mM 2-(*N*-morpholino)ethanesulfonic acid (MES) (pH 6.0) and 0.8 M sucrose were mechanically disrupted by a bead-beater (Biospec Products) at 4 °C using 0.2-mm glass beads in the presence of 1 mM phenylmethylsulfonylfluoride, 1 mM benzamidine, 1 mM ϵ-amino caproic acid, 50 μg/mL DNase, and 0.2% (w/v) BSA. Unbroken cells were separated from the thylakoid membranes by centrifugation at 1000 rpm for 10 min in a Sorvall SS34 rotor. The supernatant was then centrifuged after addition of 40 mM $CaCl_2$ at 10 000 rpm for 10 min in the SS34 rotor to collect thylakoid membranes. The final pellet was resuspended in 20 mM MES (pH 6.0), 20 mM $CaCl_2$, 20 mM $MgCl_2$, and 25% glycerol and kept frozen at −80 °C.

Preparation of Pigments. Total pigments were extracted from thylakoids by 100% methanol. The mixture was first centrifuged at 1000*g* to remove the insoluble fraction. The extract was then diluted by a factor of 4 with water before re-extracting the total pigment into hexane. The concentrated pigment in the hexane layer was dried and dissolved in methanol before injection onto a Lichrosorb RP-8 HPLC column (Alltech). The HPLC was run at 1 mL/min using methanol as the mobile phase. The eluant was monitored at 410 or 700 nm, and the Chl peak was collected. Pheo was prepared by dissolving a dried sample of purified Chl in glacial acetic acid. The acid was then evaporated under N_2 gas, and the dried Pheo pigment was dissolved in a glassing agent (4:1 ethanol/methanol mixture) prior to freezing. Measurements were made at 1.7 K in a 80 μL cell with 1 mm path length.

EPR Measurements. For these experiments, freshly harvested cells were re-suspended in fresh medium and the Chl concentration was adjusted to 0.7 mg of Chl/mL. All EPR measurements were carried out on a Bruker ESP 300E spectrometer equipped with a TM011 cavity. The sample was introduced into the EPR flat cell through a long tube kept in a water bath at 4 °C in the dark using a Gilson minipulse 3 pump. The pump speed was chosen so that each aliquot receives 12 flashes during the passage through the EPR cell. As such, the $Y_Z^{\cdot}$ decay kinetics acquired represent a uniform contribution of all S-state transitions. Saturating 10 μs xenon flashes from an EG&G electro-optic flash lamp focused through a nonmagnetic optical fiber were used to excite the sample. A nonmagnetic optical fiber was used to illuminate the sample in the EPR cavity. The ESP 300E spectrometer computer controlled the EPR data acquisition and triggering. The flash lamp was triggered within a fixed delay time after the data acquisition was started. The $Y_Z^{\cdot}$ decay kinetic measurements were performed at 8−10 °C for thylakoid membranes or room temperature for intact cells in the presence of 0.4 mM DMBQ and 1 mM $K_3Fe(CN)_6$ as the electron acceptors. From all of the $Y_Z^{\cdot}$ decay kinetics traces, a field-independent flash artifact signal measured at $g = 1.99$ was subtracted.

Chlorophyll a Fluorescence Measurements. Flash-induced Chl *a* fluorescence decay kinetics were measured at room temperature on a PAM 101 pulse-modulated Chl fluorometer (Walz, Germany). Chl fluorescence was monitored by a weak modulated light at 1.6 kHz, passed through a Corning blue filter. Samples (2 mL) of cyanobacteria cells were first treated by 40 μM 3-(3,4-dichlorophenyl)-1,1-dimethylurea (DCMU) for 10 min before addition of external electron acceptors [0.3 mM *p*-benzoquinone (PBQ) and 0.3 mM $K_3Fe(CN)_6$]. A short saturating actinic flash was provided by a xenon flash lamp to excite the cells in a 4-mL fluorescence cuvette placed in the sample chamber. The photodiode detector was protected by a Corning red filter. The data collection and averaging was done using Labview.

Low-Temperature Optical Spectroscopy. Thylakoid membranes were concentrated to 1 mg of Chl/mL and resuspended in 50 mM MES (pH 6.5), 20 mM $MgCl_2$, 20 mM $CaCl_2$, and 60% glycerol. Glycerol functions as a cryoprotectant and glassing agent. To improve the optical clarity of the sample, the mixture was solubilized for 20 min with 1% β-dodecyl-maltoside prior to glassing. The solubilized sample was freeze−thawed and briefly centrifuged to remove bubbles, before being introduced into a strain-free, quartz-windowed cell assembly of 12 mm in diameter and a path length of 0.5 mm. Glasses of high optical quality were obtained by lowering the sample rod into the liquid helium and cooling from 300 to 4 K over 30−60 s. Illuminations were performed with a 150 W quartz halogen lamp. White light from the lamp was passed through a 10 cm water filter and focused on the sample, which remained in the cryostat at low temperature. The light intensity at the sample was 100 mW/cm^2.

Table 1: Phtosystem II Donor-Side Activities in *A. marina* and *Synechocystis* PCC 6803

	O_2 activity[a]	$Y_Z^{\cdot}$ intensity[b]	$Y_Z^{\cdot}$ rereduction rate components in μs (I)[c]
A. marina	230	27	140 (0.75), 1200 (0.25)
S. 6803	270	28	140 (0.75), 1200 (0.25)

[a] Averaged activity of three different batches used for EPR experiments. The steady-state O_2 activity [μmol of O_2/(mg of Chl h)] was measured in the presence of 0.4 mM DMBQ and 0.5 mM $K_3Fe(CN)_6$ in the growth media. [b] The signal intensity at $t = 120$ μs. [c] Corresponding I_a for each component.

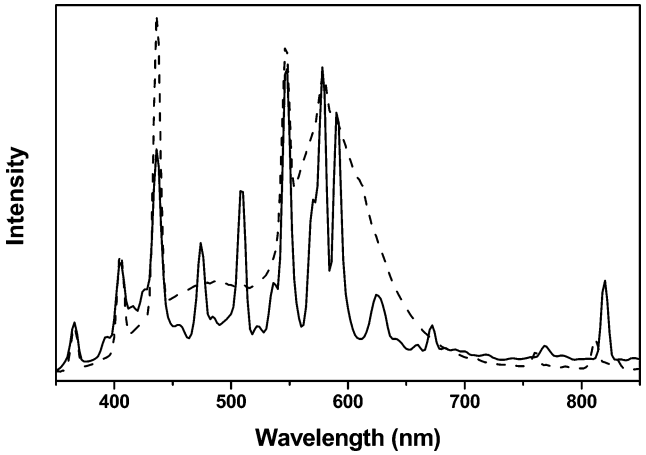

FIGURE 1: Visible spectra of arc-metal (—) and fluorescence (- - -) lights measured by a portable visible spectrophotometer.

Absorption, CD, and magnetic circular dichroism (MCD) data were simultaneously recorded on a spectrometer designed and constructed in our laboratory, as previously described (*32*, *33*). The reported spectral changes were not influenced by wavelength jitter or drift in the monochromator or actinic light. The spectra presented in this paper were recorded with 0.2-nm resolution.

RESULTS

The growth conditions of *A. marina* were optimized to increase the number of PSII centers per cell based on the Chl content, which is reflected in the steady-state O_2 evolution activity of the cells and their $Y_D^{\cdot}$ signal intensity. Light intensity and quality are known to play an important role in the PSII/PSI ratio and in the size of the light-harvesting antenna. Table 1 shows the O_2 activity of *A. marina* grown in white light at 60 μmol of photons m^{-2} s^{-1} intensity provided by a metal-arc lamp. In this light quality and intensity, the O_2 activity of cells was significantly increased compared to the typical activity of 70 (μmol of O_2/(mg of Chl h)), which was previously reported using fluorescence or incandescent lamps (*6*). See Figure 1 for a comparison of the light quality between the two types of lamps. Parts a and b of Figure 2 show the room-temperature $Y_D^{\cdot}$ EPR spectra of *A. marina* and *S.* 6803, respectively, at 4 G modulation amplitude. Consistent with the O_2 activity (Table 1), the $Y_D^{\cdot}$ signal intensity of *A. marina* was also comparable with that of *S.* 6803.

To obtain quality $Y_Z^{\cdot}$ decay signals from intact cells, EPR experimental parameters were first optimized. Improvement of the signal-to-noise (S/N) ratio is a prerequisite to a successful extraction of the $Y_Z^{\cdot}$ kinetic parameters because

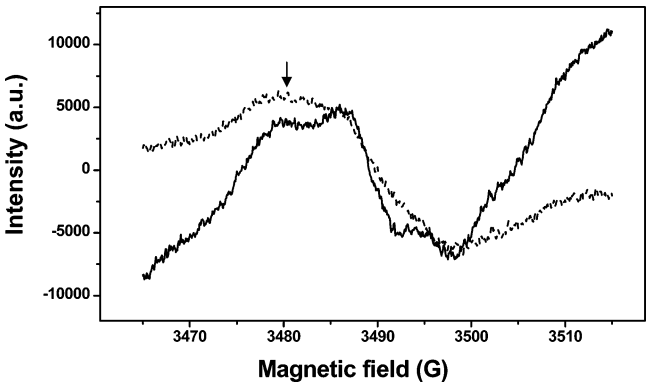

FIGURE 2: $Y_D^{\cdot}$ spectra of *A. marina* (—) and *S.* 6803 cells (- - -). Arrow indicates the field position at which $Y_Z^{\cdot}$ decay kinetics were measured. The underlying signal seen in the $Y_D^{\cdot}$ spectrum of *A. marina* is due to the high content of Mn taken up by cells grown under high light conditions (*56*). Instrumental parameters: 20 mW, microwave power; 4 G, modulation amplitude; 100 kHz, modulation frequency; 9.7920 GHz, microwave frequency; and 82 ms, time constant. To compare signal intensities, samples were treated with EDTA to suppress the Mn six-line signal (*56*).

the detected signal from intact cells suffers from a poor S/N ratio. The poor S/N is due to the inherent noise associated with the use of a fast instrument response time necessary to detect the $Y_Z^{\cdot}$ signal that rises and decays rapidly (*34*−*39*). Because the sensitivity is of prime concern for the kinetic measurements, the modulation amplitude can be adjusted to maximize the signal intensity. Although overmodulation increases the signal intensity, it also decreases the spectral resolution.

Common to biological EPR signals, asymmetry in the spectrum arises because the signal is an envelope of overlapping individual hyperfine components of Gaussian line shape with narrower intrinsic line widths. For Gaussian lines, the maximum amplitude is usually obtained when the modulation amplitude is set to about the peak-to-peak derivative line width. For the $Y_Z^{\cdot}$ spectrum and accordingly the $Y_D^{\cdot}$ spectrum, when the modulation amplitude is increased from 4 to 10 G, the spectral hyperfine structure is lost because signals are somewhat overmodulated but the signal intensity was increased by a factor of ~3 (data not shown). Interestingly, the P_{700}^{+} signal, a PSI-originated EPR signal, which appears downfield from the $Y_D^{\cdot}$ signal, is still negligible even at 10 G modulation amplitude.

In previous studies, modulation amplitudes of 4−6 G were used to acquire the $Y_Z^{\cdot}$ decay kinetic (*35*, *40*−*42*). To show that such an increase in the modulation amplitude to 10 G does not result in a detectable contamination of the $Y_Z^{\cdot}$ kinetic with P_{700}^{+} kinetic components, experiments were also performed in the presence of DCMU. Such concerns were always the basis for limiting the modulation amplitude in earlier studies. Parts a and b of Figure 3 show $Y_Z^{\cdot}$ decay kinetic data taken at 4 and 10 G modulation amplitude, respectively, on the same spinach thylakoid samples. When thylakoid samples were inhibited by DCMU, which blocks PSII ET from Q_A^{-} to Q_B, the $Y_Z^{\cdot}$ signal is completely abolished, while the intensity of the P_{700}^{+} signal is unaffected (Figure 3c). These results clearly show that the $Y_Z^{\cdot}$ decay kinetics measured by 10 G modulation amplitude is free of the P_{700}^{+} signal contribution. However, the comparison of the $Y_Z^{\cdot}$ decay kinetic data shows that an improvement of the S/N ratio by a factor of 3 was achieved by increasing the modulation amplitude from 4 to 10 G.

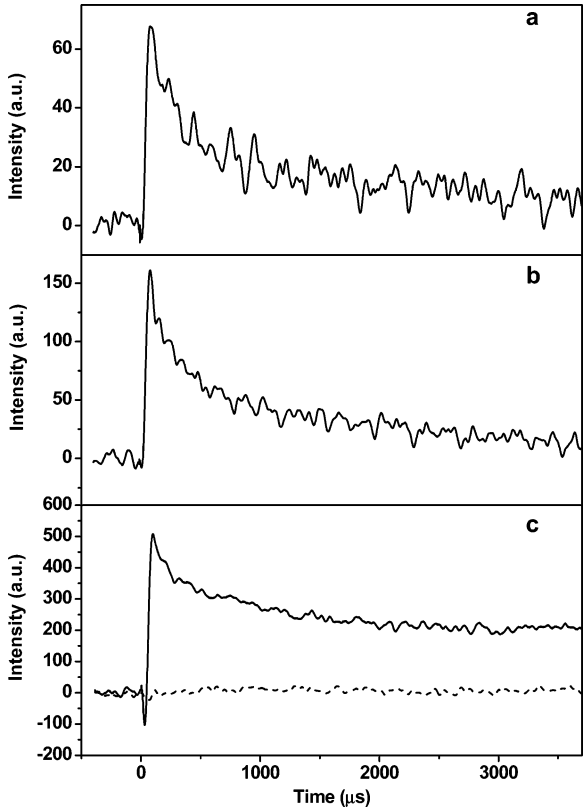

FIGURE 3: $Y_Z^{\cdot}$ and P_{700}^{+} decay kinetics of dark-adapted spinach thylakoids with a Chl concentration of 1.5 mg/mL. The sample was continuously circulated through the EPR cell such that each aliquot received 12 flashes during passage through the cavity. The Y_Z×e1$^{\cdot}$ signal represents a uniform contribution of all S-state transitions. (a) $Y_Z^{\cdot}$ decay kinetics taken using 4 G modulation amplitude, averaged for 10 000 events. (b) $Y_Z^{\cdot}$ decay kinetics taken using 10 G modulation amplitude, averaged for 5000 events. (c) P_{700}^{+} (—) and $Y_Z^{\cdot}$ (- - -) decay kinetics recorded using 10 G modulation amplitude in the presence of DCMU, averaged of 1000 and 5000 events, respectively. The magnetic field positions were 3479 and 3488 G for $Y_Z^{\cdot}$ and P_{700}^{+} decay kinetics, respectively. The P_{700}^{+} decay kinetics at this field position contain some contributions from the $Y_Z^{\cdot}$ signal because of overlapping and the CIDEP that appears as a negative spike. Signal intensities are divided by the number of averaged events. Instrumental parameters: modulation frequency, 100 kHz; microwave power, 100 mW; time constant, 20 μs; and frequency, 9.7926 GHz.

Parts a and b of Figure 4 show the $Y_Z^{\cdot}$ decay kinetic traces of *A. marina* with high O_2 activity and *S.* 6803, respectively, measured using 10 G modulation amplitude. To allow a comparison of the $Y_Z^{\cdot}$ signal intensity, the signals were divided by the number of flashes and normalized to the $Y_D^{\cdot}$ signal intensities shown in Figure 2. This is because the preilluminated $Y_D^{\cdot}$ signal intensity is directly related to the number of PSII centers because there is only one Y_D per PSII center. For the $Y_Z^{\cdot}$ traces, the rise represents the oxidation of Y_Z by the oxidized PSII primary electron donor (P^+), while the decay represents the electron donation by the Mn_4Ca cluster to $Y_Z^{\cdot}$ through S-state transitions, i.e.,

$$S_iY_ZP^+ \overset{K_{zp}}{\rightleftharpoons} S_iY_Z{}^+P \overset{K_{sz}}{\rightleftharpoons} S_{i+1}Y_ZP \qquad (1)$$

The overall reaction represents the oxidation of the Mn_4-Ca cluster advancing from the S_n-S_{n+1} state by P^+. The rise and decay of the $Y_Z^{\cdot}$ signal is then determined by the K_{zp} and K_{sz} equilibrium constants, respectively. The decay rate

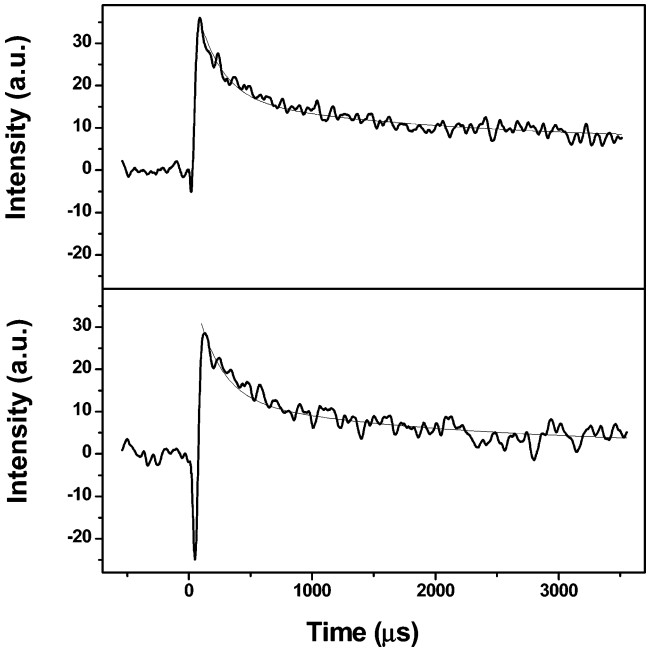

FIGURE 4: $Y_Z^{\cdot}$ decay kinetics and fit for *A. marina* (top) and *S.* 6803 cells (bottom). The signal intensities are normalized to the $Y_D^{\cdot}$ signal intensities shown in Figure 2 and divided by the number of summed events, 20 000 for *A. marina* and 11 000 for *S.* 6803.

of $Y_Z^{\cdot}$ is estimated by the least-squares fit of the data to following equation:

$$I_i(t) = I_a e^{-t/\tau_a} + I_s e^{-t/\tau_s} \qquad (2)$$

I_a and τ_a are the signal amplitude and decay time constant, respectively, for a given S state in O_2-evolving centers. I_s and τ_s represent the signal amplitude and decay time constant for a fixed fraction (10%) of inactive centers that turnover with a decay time constant of ~10 ms. The slow decaying component is that part of the signal that fails to recover during the 4 ms of data acquisition and appears as a baseline offset. Because of the fact that the $Y_Z^{\cdot}$ decay kinetics was obtained under repetitive flash conditions, the transient is assumed to reflect equal contributions of $Y_Z^{\cdot}$ reduction by each of the four S-state transitions. A two-component fit was then used to account for 75 and 25% contribution of earlier S-state transitions and the final S_3-S_0 transition, respectively. This was based on earlier kinetic data that showed that the $Y_Z^{\cdot}$ reduction rate for the early individual S-state transitions in spinach thylakoids occurs much faster (tens of microseconds) than the final S_3-S_0 transition (0.75 ms) (*38*). The smooth curves in Figure 4 represent the two-component fit with derived half-times given in Table 1.

These half-time values for *S.* 6803 are in good agreement with previous data (*22*). The decay rates appear to be very similar for *A. marina* and *S.* 6803, which is an indication of similarity of the water-oxidizing enzyme in both organisms. The final S_3-S_0 transition rate, in particular, is a good indicator for probing the Mn_4Ca cluster because it is closely coupled with the release of O_2 (*24*). This result implies that $Y_Z^{\cdot}$ functions normally in *A. marina* with the same efficiency as in *S.* 6803, meaning that the reduction potential of $Y_Z^{\cdot}/Y_Z$ is not significantly different between the two organisms. Moreover, the normalized amplitudes of the $Y_Z^{\cdot}$ signal are similar in both *A. marina* and *S.* 6803. This strongly suggests

that P^+ in *A. marina* oxidizes $Y_Z^{\cdot}$ as efficiently as *S.* 6803. Considering a similar reduction potential of $Y_Z^{\cdot}/Y_Z$ in both species, the reduction potential of P^+/P in *A. marina* is likely to be similar to that of P_{680}^+/P_{680} in *S.* 6803. If, on the other hand, the reduction potential of P^+/P in *A. marina* was more negative than P_{680}^+/P_{680}, it would approach the reduction potential of $Y_Z^{\cdot}/Y_Z$ and Y_Z could no longer be an efficient electron donor to P^+. It was experimentally shown that when the reduction potential of P_{680}^+/P_{680} is decreased by −43 or −82 mV, 9−32% of P_{680}^+ remains oxidized at $t > 200$ μs (*43*). However, a loss with such magnitude was not observed for the $Y_Z^{\cdot}$ signal amplitude (Table 1). To be able to perform the signal intensity analysis at $t < 120$ μs, the $Y_Z^{\cdot}$ signal of *A. marina* at 85 μs was also compared to that of spinach thylakoid (Figure 2b), where the chemically induced dynamic electron polarization signal (CIDEP) is less pronounced. On the basis of $Y_Z^{\cdot}$ reduction rates given in Table 1, this amplitude at 85 μs corresponds to 70% of the total $Y_Z^{\cdot}$ signal. Even though 30% of the signal was not detected because of the presence of CIDEP and the EPR time constant, the remaining 70% still represents an average of all S states with 45% contribution from the first three S-state transitions. The corresponding normalized amplitudes were 36 and 37 for *A. marina* and spinach thylakoids, respectively. This also strengthens the argument that the reduction potential of P^+/P in *A. marina* is likely to be similar to that of higher plants. However, the $Y_Z^{\cdot}$ amplitude differences up to 10% could have escaped detection because of the S/N ratio limiting our analysis for small changes in the reduction potential. Fluorescence experiments were then performed to further characterize the system.

If the reduction potential of P^+/P in *A. marina* is more negative than P_{680}^+/P_{680}, then the steady-state population of P^+ would also be different and hence should have a significant effect on the rate of charge recombination. The rate of charge recombination can be monitored by the decay in the variable Chl fluorescence yield after flash illumination, which is governed by the level of reduced Q_A. Redox species that quench fluorescence and impact the yield are the primary electron donor and the plastoquinone pool. The kinetics of increase of the fluorescence induction curve are also affected by the connectivity of the light-harvesting antenna to the PSII reaction center and energy transfer between centers (*44*). In the time range of millisecond−seconds at room temperature, several components in the fluorescence decay can be observed (*45*). The fast components are due to the loss of Q_A^- by forward ET to Q_B and the reduction of the plastoquinone pool. However, in the presence of DCMU, forward ET is blocked and the reoxidation of Q_A^- and the decline in the variable fluorescence are primarily due to charge recombination between Q_A^- and the PSII donor side (*43*). Variations in the fluorescence yield because of the antenna size and the exciton equilibration with the primary radical pair are not significant over the millisecond−second time range when Q_A is in a fully closed state (*46*). Thus, under these conditions, the fluorescence decay reflects mainly the rate of recombination and the relative concentration of P^+ following the equilibration with the S states and $Y_Z^{\cdot}$, as shown in reaction 1. This means that as P^+ gets more populated, the observed rate of charge recombination becomes faster.

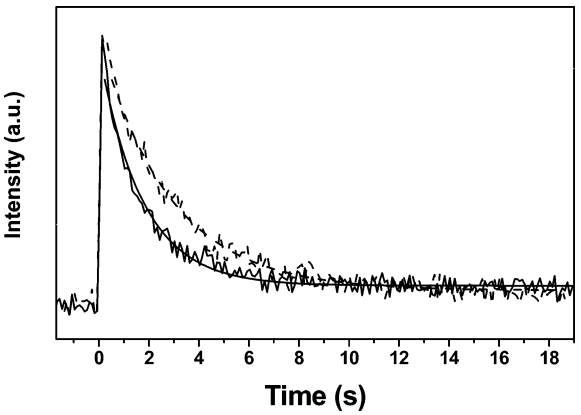

FIGURE 5: Flash-induced Chl *a* fluorescence decay kinetics and fit in *A. marina* (—) and *S.* 6803 cells (- - -) in the presence of 40 μM DCMU. All measurements were performed at room temperature, and each signal is an average of 10 traces. The signal intensity for *S.* 6803 was normalized to that of *A. marina*.

Figure 5 shows the fluorescence decay kinetics for *A. marina* and *S.* 6803 cells that were dark-adapted for 10 min in the presence of PBQ, $K_3Fe(CN)_6$, and DCMU. The dark adaptation with PBQ and $K_3Fe(CN)_6$ ensures that the plastoquinone pool is oxidized and that acceptor side of PSII starts in the Q_AQ_B state (*43*). A monoexponential decay was fit to the data in Figure 5 and gave rate constants of 0.59 and 0.37 s^{-1} for *A. marina* and *S.* 6803, respectively. Assuming a similar intrinsic rate constant for both species and simplifying the observed fluorescence decay kinetics by relating it to only redox species (eq 1), the difference in reduction potential between P^+/P in *A. marina* and P_{680}^+/P_{680} ($\Delta E'$) can be estimated by eq 3

$$\Delta E' = 59 \log(K_{zp}/K_{zp680}) \qquad (3)$$

K_{zp} and K_{zp680}, which are directly related to the rate constants, are the equilibrium constants given in eq 1 for *A. marina* and *S.* 6803, respectively. The charge recombination rate is also strongly dependent on the free-energy gap between P^+ and $Pheo^-$ (*47*). The Pheo type in *A. marina* was therefore identified by optical spectroscopy and shown to be Pheo *a* (see below). A similar redox potential for Pheo is then expected in both species allowing the application of eq 3 and its relation to the reduction potential of P^+/P. The resulting estimated $\Delta E'$ value is only about −10 mV, thus supporting the conclusion drawn from the EPR measurements that the reduction potential of P^+/P in *A. marina* is similar to that of P_{680}^+/P_{680} in *S.* 6803. It is worth noting that a $\Delta E'$ value of −100 mV translates into a 75 times faster recombination rate for a modified reaction center (*43*).

In another approach to characterize the reaction center of PSII in *A. marina*, the Pheo type in *A. marina* was identified by optical spectroscopy. The lower trace in Figure 6 shows the low-temperature absorption spectrum of a thylakoid sample of *A. marina* in the 540−560 nm range. Absorption features in this region are mainly due to cytochromes such as cyt b_{559} and b_6f and bc_1 complexes. Weak features associated with the Q_x absorbance of Pheo *a* can also be observed in this spectral region in purified PSII samples (*28*) but are masked in the spectra of thylakoid samples by the large number of cytochromes present. The upper trace in Figure 6 presents the difference spectrum after low-temper-

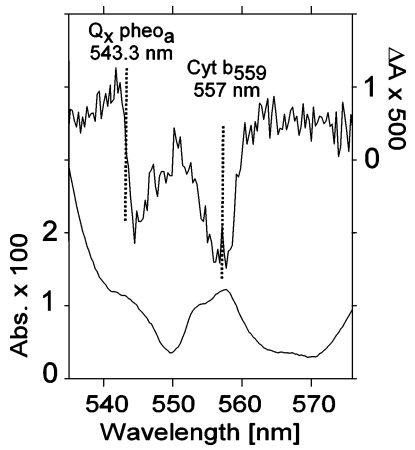

FIGURE 6: Lower trace (left-hand scale), low-noise absorption spectrum of *A. marina* thylakoids in 50% glycerol at 1.7 K in the Cyt and Pheo Q_x absorption region. A linear background was subtracted from the spectrum. Upper trace (right-hand scale), change in absorption in lower trace after illumination at 1.7 K for 5 min with white light (see the text).

ature illumination. This provides a clear PSII/ Q_A^- formation signature in *A. marina*. The "C550" differential feature is at 543.3 nm, and there is a parallel bleach at 557 nm. These features are analogous to those seen for PSII membranes and core complexes (*28*). The bleach feature at 557 nm is assigned to oxidation of the reduced form of cyt b_{559} based on the presence of an MCD A term at this spectral position *before* illumination (data not shown). The corresponding reduced cyt b_{559} absorption in spinach PSII membranes is at 556 nm (*28*).

The "C550" feature at 543.3 nm, which is due to an electrochromic shift on the redox-active Pheo induced by Q_A^- formation, clearly identifies the redox-active Pheo in *A. marina*. Parallel studies of the low-temperature illumination of *S.* 6803 thylakoids show no corresponding C550 feature, because PSII spectral features in such preparations are completely masked by inherently high PSI/PSII ratios in *S.* 6803. However, there is a close correspondence of the *A. marina* C550 feature (543.3 nm) with that of Pheo *a* in PSII fragments (545.4 nm) and in *S.* 6803 PSII core complexes (542 nm). This is an indicator that the redox-active Pheo is Pheo *a*. Furthermore, we were able to identify a Q_y electrochromic feature in *A. marina* at 692 nm. In PSII membranes and *S.* 6803 core complexes, the Q_y−Pheo *a* feature occurs at 683.5 and 684.1 nm, respectively (*28*). These similarities immediately point to the likelihood that the redox-active Pheo in *A. marina* is indeed Pheo *a*. To eliminate Pheo *d* as a possibility, the low-temperature absorption and MCD of both Pheo *a* and *d* were measured to compare their Q_x and Q_y positions. Spectra of Chl *a* and Pheo *a* agree with previous room-temperature solution measurements (*48*), although our low-temperature spectra are better resolved. Figure 7 shows the low-temperature spectra of Pheo *d* and Chl *d*, not previously reported. The absorption data in Figure 7 for Chl *d* agree with 170 K data in methanol/acetonitrile (*13*) with our main peak at 701 nm compared to 699 nm. However, from its clear negative MCD signature, the peak at 672 nm is unlikely to be a chlorin impurity as suggested (*13*). An impurity Q_y band would have a positive MCD B term. We suggest the band is due to Q_y (1, 0) in analogy to a similar band in Chl *a*, and the second negative

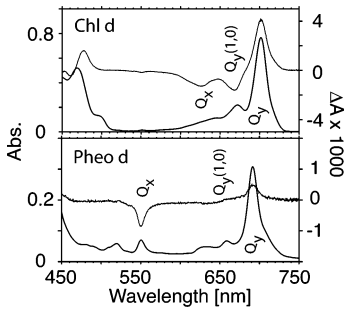

FIGURE 7: Absorption (lower trace, left-hand scale) and MCD at 5T (upper trace, right-hand scale) of Pheo *d* (lower panel) and Chl *d* (upper panel), both in a 4:1 (v/v) ethanol/methanol glass measured at 1.7 K. Assignments of the Q_x and Q_y features are indicated, determined from their MCD characteristics.

MCD feature identifies Q_x as being near 626. The MCD spectra in particular allow a clear assignment of both Q_x and Q_y transitions in these pigments. As it is shown in Figure 7, Pheo *d* has a Q_y band at 691.5 nm and a clear negative MCD Q_x band at 550.5 nm. In comparison, Q_y and Q_x of Pheo *a* are positioned at 667.5 and 537.6 nm, respectively, measured in the same solvents/glassing mixture. The redox-active Pheo observed in *A. marina* (543.3 nm) is then very unlikely to be Pheo *d*, because this would require a blue shift of ∼7 nm from the position observed for free Pheo *d*. It is well-known (*49*) that spectral shifts in chlorin Q_x transitions are dominated by axial ligation effects. Pheo *d*, not having a central metal involved in axial ligation, cannot have its Q_x transition affected in this way. Q_x can be expected to experience a typical ∼10−20 nm red shift, seen for many chlorins in a protein environment.

DISCUSSION

In this study, we have found that the low O_2 evolution of *A. marina* cells [typically 70 μmol of O_2 (mg of Chl)$^{-1}$ h^{-1}] could be increased by a factor of 3 when cells are grown under high-light conditions using metal-arc lamps (Table 1). This provided a major improvement in the S/N ratio for the $Y_Z^{\cdot}$ EPR measurements of whole cells, which were used to extract kinetic parameters. We also compared the PSI content for the samples grown under low (10 μmol of photons m^{-2} s^{-1}) and high (60 μmol of photons m^{-2} s^{-1}) light conditions using a P_{740}^+ EPR signal. The PSI content decreased by half when the cells were grown in high light (data not shown), while specific O_2 activity was significantly increased (Table 1). The lower O_2 activity observed in previous studies of *A. marina* could be interpreted as the result of slow O_2 release from the oxygen-evolving complex (OEC) in *A. marina* caused by a lower oxidation potential of $Y_Z^{\cdot}/Y_Z$ and P^+/P. Rather, the high O_2 activity reported here, together with $Y_Z^{\cdot}$ decay kinetics, strongly suggests that the OEC functions normally in *A. marina* and that the O_2 release rate is essentially the same (*24*). To our knowledge this provides the first evidence that the water oxidation mechanism in *A. marina* is kinetically similar to that in *S.* 6803 and spinach thylakoids.

It is now clear that Chl *d* is the major Chl type in *A. marina* and forms the primary electron donor of the PSI complex in this organism (*7*, *8*); however, there has been a debate on the identity of the primary donor of PSII. The EPR and

fluorescence measurements reported here (Figures 4 and 5) on whole cells support the idea that the physicochemical properties of the primary electron donor of *A. marina* are not much different than those of the Chl *a* primary electron donor of the well-studied cyanobacterium *S.* 6803. If we assume that the primary electron donor of PSII in *A. marina* is Chl *d*, then a decrease by more than −160 mV in the oxidation potential of P^+/P might be expected in comparison to the Chl *d*-type PSI complex, unless the properties of the PSII primary electron donor are compensated by other factors in the protein environment.

It is well-known that the protein environment plays a crucial role in the properties of primary electron donors, which are photo-oxidizable, as opposed to the Chl's in the antenna system, which are not. For example, even though the primary electron donors of PSI and PSII in most organisms are composed of Chl *a* molecules, their oxidation potentials are quite different. The properties of the various Chl types are believed to be controlled by the protein backbone, which organizes the Chl molecules in relation to each other and interacts directly with the Chl side chains to provide a low dielectric environment. The importance of the protein environment on the oxidation potential of the primary donor has been shown by modifying the natural system through site-directed mutagenesis. For example, it was shown that the formation of up to four hydrogen bonds with the bacterial primary electron donor could additively increase the oxidation potential by a remarkable 335 mV (*50*, *51*), enough to raise the redox poise to oxidize a tyrosine residue, which is the primary requirement for water oxidation in PSII (*52*). Likewise, the midpoint potential for P_{680} in *S.* 6803 could also be changed but to a lesser extent, by introducing a series of site-directed mutations at D1-His198 and D2-His197 ligation sites (*43*). These histidine residues are conserved in *A. marina*, which shows a high degree of homology (up to 93%) in the D1 and D2 proteins between *A. marina* and *S.* 6803 (*4*, *8*).

If the primary donor of PSII in *A. marina* is made up of Chl *a* and not Chl *d*, then the charge-separated state of PSII will be near 680 nm and an uphill energy transfer would have to occur *in vivo* to connect with the Chl *d*-containing, light-harvesting pigment−proteins, which absorb lower energies at longer wavelengths. Such an uphill energy transfer was originally suggested by Mimuro et al. (*53*), although it has been challenged by Nieuwenburg et al. (*13*) based on an investigation of the absorption and emission properties of isolated Chl *d*. However, there is accumulating evidence (*54*, *55*) that the charge separating state of PSII (in spinach) lies at significantly lower energy than conventionally believed (>700 nm rather than at 680 nm). Such a low-energy charge-separating state could facilitate any uphill energy transfer in *A. marina* at ambient temperatures if Chl *a* is the primary donor.

Additionally, Mimuro et al. (*5*) have recently used fluorescence studies of *A. marina* cells together with pigment analysis of the whole cells grown under three different light intensities to support their assignment of the PSII primary electron donor to Chl *a*. When cells are grown under very low light intensity (5 μmol of photons m^{-2} s^{-1}), the Chl *a* content decreases to Chl *a*/Pheo *a* = 1. Thus, it was suggested that two Chl *a* molecules (specifically forming the dimeric Chl pair) act as the primary electron donor, while the accessory Chl's in the RC are Chl *d* molecules. This would mean that the D1 and D2 polypeptides are modified such that they can bind two different types of Chl's. From the ratio of Chl *d*/Chl *a* [65 in low light (*5*)], one can conclude that the D1 and D2 polypeptides in PSII must have a very high specificity toward Chl *d*, except for the particular sites associated with the primary electron donor. The binding affinity for Chl *a* at the other sites would be relatively low. If this is the case, there would be certain amino acid substitutions to allow selectivity for a given binding site. However, from sequence alignment studies, such amino acid substitutions are not apparent in D1 and D2.

From illumination-induced electrochromism experiments performed in this work, we have shown that Pheo *a* is the redox-active Pheo in *A. marina*, which had not previously been established directly. This assignment arises because both the spectral position and phenomenology of the electrochromism in *A. marina* parallels the behavior observed in well-studied PSII systems with Pheo *a* in their reaction centers. However, the quantum efficiency of the low-temperature photoreduction of the plastoquinone, which is 0.1 in higher plants and *S.* 6803 core complexes (*28*), is ∼100 times less efficient in *A. marina*. At low temperatures, illumination doses that gave rise to complete conversion to the $S_1(Q_A^-)$ state in plant thylakoid and other PSII samples lead to negligible conversion in *A. marina* thylakoid samples, consistent with inhibited uphill energy transfer to the charge-separating state at low temperatures.

In summary, there are still two possibilities to explain the properties of the primary electron donor of PSII in *A. marina*: (1) the primary donor consists of Chl *a* molecules similar to P_{680} in higher plants and other cyanobacteria, or (2) the primary donor consists of Chl *d* molecules (a novel type) whose properties are determined by a special protein environment. To gain a better insight of Chl−protein interactions, the development of model Chl-binding protein maquettes is underway in our group in which the Chl-binding sites can be modified for tuning the properties of bound Chl *a* and Chl *d*.

ACKNOWLEDGMENT

We thank Dr. Warwick Hillier and Dr. Ronald Steffen for helpful discussions.

REFERENCES

1. Deisenhofer, J., Epp, O., Miki, K., Huber, R., and Michel, H. (1985) Structure of the protein subunits in the photosynthetic reaction center of *Rhodopseudomonas viridis* at 3 Å resolution, *Nature 318*, 618−624.
2. Miyashita, H., Ikemoto, H., Kurano, N., Adachi, K., Chihara, M., and Miyachi, S. (1996) Chlorophyll *d* as a major pigment, *Nature 383*, 402.
3. Blankenship, R. E., and Hartman, H. (1998) The origin and evolution of oxygenic photosynthesis, *Trends Biochem. Sci. 23*, 94−97.
4. Miyachita, H., Ikemoto, H., Kurano, N., and Miyachi, S. (2003) *Acaryochloris marina* Gen. et. sp. nov. (cyanobacteria), an oxygenic photosynthetic prokaryote containing chl *d* as a major pigment, *J. Phycol. 39*, 1247−1253.
5. Mimuro, M., Akimoto, S., Gotoh, T., Yokono, M., Akiyama, M., Tsuchiya, T., Miyashita, H., Kobayashi, M., and Yamazaki, I. (2003) Identification of the primary electron donor in PS II of the Chl *d*-dominated cyanobacterium *Acaryochloris marina*, *FEBS Lett. 27933*, 1−4.

6. Boichenko, V. A., Klimov, V. V., Miyashita, H., and Miyachi, S. (2000) Functional characteristics of chlorophyll *d*-predominating photosynthetic apparatus in intact cells of *Acaryochloris marina*, *Photosynth. Res. 65*, 269−277.
7. Hu, Q., Miyashita, H., Iwasaki, I., Kurano, N., Miyachi, S., Iwaki, M., and Itoh, S. (1998) A photosystem I reaction center driven by chlorophyll *d* in oxygenic photosynthesis, *Proc. Natl. Acad. Sci. U.S.A. 95*, 13319−13323.
8. Akiyama, M., Miyashita, H., Kise, H., Watanabe, T., Miyachi, S., and Kobayashi, M. (2001) Detection of chlorophyll *d*′ and pheophytin *a* in a chlorophyll *d*-dominating oxygenic photosynthetic prokaryote *Acaryochloris marina*, *Anal. Sci. 17*, 205−208.
9. Golbeck, J. H., and Bryant, D. A. (1991) Photosystem-I, *Curr. Top. Bioenerg. 16*, 83−177.
10. Brettel, K. (1997) Electron transfer and arrangement of the redox cofactors in photosystem I, *Biochim. Biophys. Acta 1318*, 322−373.
11. Mimuro, M., Akimoto, S., Yamazaki, I., Miyashita, H., and Miyachi, S. (1999) Fluorescence properties of chlorophyll *d*-dominating prokaryotic alga, *Acaryochloris marina*: Studies using time-resolved fluorescence spectroscopy on intact cells, *Biochim. Biophys. Acta 1412*, 37−46.
12. Itoh, S., Iwaki, M., Noguti, T., Kawamori, A., Mino, H., Hu, Q., Iwasaki, I., Miyashita, H., Kurano, K. N., Miyachi, S., and Shen, R. (2001) in *Proceedings of the 12th International Congress on Photosynthesis*, pp S6−S28.
13. Nieuwenburg, P., Clarke, R. J., Cai, Z. L., Chen, M., Larkum, A. W. D., Cabral, N. M., Ghiggino, K. P., and Reimers, J. R. (2003) Examination of the photophysical processes of chlorophyll *d* leading to a clarification of proposed uphill energy transfer processes in cells of *Acaryochloris marina*, *Photochem. Photobiol. 77*, 628−637.
14. Kok, B., Forbush, B., and McGloin, M. (1970) Cooperation of charges in photosynthetic O_2 evolution I. A linear four step mechanism, *Photochem. Photobiol. 11*, 457−475.
15. Joliot, P., Barbieri, G., and Chabaud, R. (1969) Un nouveau modele des centers photochimiques du systeme II, *Photochem. Photobiol. 10*, 309−329.
16. Debus, R. J., Barry, B. A., Sithole, I., Babcock, G. T., and McIntosh, L. (1988) Direct mutagenesis indicates that the donor to P_{680}^+ in photosystem II is tyrosine-161 of the D1 polypeptide, *Biochemistry 27*, 9071−9074.
17. Metz, J. G., Nixon, P. J., Rögner, M., Brudvig, G. W., and Diner, B. A. (1989) Directed alternation of the D1 polypeptide of photosystem II: Evidence that tyrosine-161 is the redox component, Z, connecting the oxygen-evolving complex to the primary electron donor, P_{680}, *Biochemistry 28*, 6960−6969.
18. Blankenship, R. E., Babcock, G. T., Warden, J. T., and Sauer, K. (1975) Observation of a new EPR transient in chloroplasts that may reflect the electron donor to photosystem II at room temperature, *FEBS Lett. 51*, 287−293.
19. Warden, J. T., Blankenship, R. E., and Sauer, K. (1976) A flash photolysis ESR study of photosystem II signal II_{vf}, the physiological donor to P_{680}, *Biochim. Biophys. Acta 423*, 462−478.
20. Vermaas, W. F. J., Rutherford, A. W., and Hansson, Ö. (1988) Site-directed mutagenesis in photosystem II of the cyanobacterium *Synechocystis* sp. PCC 6803: Donor D is a tyrosine residue in the D2 protein, *Proc. Natl. Acad. Sci. U.S.A. 85*, 8477−8481.
21. Babcock, G. T., and Sauer, K. (1975) A rapid, light-induced transient in electron paramagnetic resonance signal II activated upon inhibition of photosynthetic oxygen evolution, *Biochim. Biophys. Acta 376*, 315−328.
22. Razeghifard, M. R., Wydrzynski, T., Pace, R. J., and Burnap, R. L. (1997) $Y_z^{\cdot}$ reduction kinetics in the absence of the manganese-stabilizing protein of photosystem II, *Biochemistry 36*, 14474−14478.
23. Razeghifard, M. R., and Pace, R. J. (1997) Electron paramagnetic resonance kinetics studies of the S states in spinach PSII membranes, *Biochim. Biophys. Acta 1322*, 141−150.
24. Razeghifard, M. R., and Pace, R. J. (1999) EPR kinetic studies of oxygen release in thylakoids and PSII membranes: A kinetic intermediate in the S_3 to S_0 transition, *Biochemistry 38*, 1252−1257.
25. Mulkidjanian, A. Y., Cherepanov, D. A., Haumann, M., and Junge, W. (1996) Photosystem II of green plants: Topology of core pigments and redox cofactors as inferred from electrochromic difference spectra, *Biochemistry 35*, 3093−3107.
26. van Gorkom, H. (1974) Identification of the reduced primary electron acceptor of photosystem II as a bound semiquinone anion, *Biochim. Biophys. Acta 347*, 439−442.
27. Butler, W. L. (1971) The photoproduction of *C-550* in chloroplasts and its inhibition by lipase, *Biochim. Biophys. Acta 245*, 237−239.
28. Peterson Årsköld, S., Masters, V. M., Prince, B. J., Smith, P. J., Pace, R. J., and Krausz, E. (2003) Optical spectra of *Synechocystis* and spinach photosystem II preparations: Identification of the D1-pheophytin energies and stark shifts, *J. Am. Chem. Soc. 125*, 13063−13074.
29. Porra, R. J., Thompson, W. A., and Kriedemann, P. E. (1989) Determination of accurate extinction coefficients and simultaneous equations for assaying chlorophylls *a* and *b* extracted with four different solvents: Verification of the concentration of chlorophyll standards by atomic absorption spectroscopy, *Biochim. Biophys. Acta 975*, 384−394.
30. Chen, M., Quinnell, R. G., and Larkum, A. W. D. (2002) Chlorophyll *d* as the major photopigment in *Acaryochloris marina*, *J. Porphyrins Phthalocyanines 6*, 763−773.
31. Razeghifard, M. R., Kim, S., Patzlaff, J. S., Hutchison, R. S., Krick, T., Ayala, I., Steenhuis, J. J., Boesch, S. E., Wheeler, R. A., and Barry, B. A. (1999) *In vivo*, *in vitro*, and calculated vibrational spectra of plastoquinone and the plastosemiquinone anion radical, *J. Phys. Chem. B 103*, 9790−9800.
32. Smith, P. J., Peterson, S., Masters, V. M., Wydrzynski, T., Styring, S., Krausz, E., and Pace, R. J. (2002) Magneto-optical measurements of the pigments in fully active photosystem II core complexes from plants, *Biochemistry 41*, 1981−1989.
33. Stranger, R., Dubicki, L., and Krausz, E. (1996) Magneto-optical investigation of the exchange-coupled dimer $Cs_3Mo_2Br_9$, *Inorg. Chem. 35*, 4218−4226.
34. Boska, M., Blough, N. V., and Sauer, K. (1985) The effect of mono- and divalent salts on the rise and decay kinetics of EPR signal II in photosystem II preparations from spinach, *Biochim. Biophys. Acta 808*, 132−139.
35. Babcock, G. T., Blankenship, R. E., and Sauer, K. (1976) Reaction kinetics for positive charge accumulation on the water side of chloroplast photosystem II, *FEBS Lett. 61*, 286−289.
36. Boska, M., Sauer, K., Buttner, W., and Babcock, G. T. (1983) Similarity of EPR signal II_f rise and P_{680}^+ decay kinetics in tris-washed chloroplast photosystem II preparation as a function of pH, *Biochim. Biophys. Acta 722*, 327−330.
37. Debus, R. J. (1992) The manganese and calcium ions of photosynthetic oxygen evolution, *Biochim. Biophys. Acta 1102*, 269−352.
38. Razeghifard, M. R., Klughammer, C., and Pace, R. J. (1997) Electron paramagnetic resonance kinetic studies of the S states in spinach thylakoids, *Biochemistry 36*, 86−92.
39. Renger, G. (2001) Photosynthetic water oxidation to molecular oxygen: Apparatus and mechanism, *Biochim. Biophys. Acta 1503*, 210−228.
40. Cole, J., and Sauer, K. (1987) The flash number dependence of EPR signal II decay as a probe for charge accumulation in photosystem II, *Biochim. Biophys. Acta 891*, 40−48.
41. Hoganson, C. W., and Babcock, G. T. (1988) Electron-transfer near the reaction center in O_2-evolving photosystem II preparations, *Biochemistry 27*, 5848−5855.
42. Lydakis-Simantiris, N., Hoganson, C. W., Ghanotakis, D. F., and Babcock, G. T. (1995) in *Photosynthsis: From Light to Biosphere* (Mathis, P., Ed.) pp 279−282, Kluwer Academic Publishers, Dordrecht, The Netherlands.
43. Diner, B. A., Schlodder, E., Nixon, P. J., Coleman, W. J., Rappaport, F., Lavergne, J., Vermass, W. F. J., and Chisholm, D. A. (2001) Site-directed mutations at D1-His198 and D2-His197 of photosystem II in *Synechocystis* PCC 6803: Sites of primary charge separation and cation and triplet stabilization, *Biochemistry 40*, 9265−9281.
44. Diner, B. A. (1998) Application of spectroscopic techniques to the study of photosystem II mutations engineered in *Synechocystis* and *Chlamydomonas*, *Methods Enzymol. 297*, 337−360.
45. Renger, G., Eckert, H.-J., Bergmann, A., Bernarding, J., Liu, B., Napiwotzki, A., Reifarth, F., and Eichler, H. J. (1995) Fluorescence and spectroscopic studies of exciton trapping and electron transfer in photosytem II of higher plants, *Aust. J. Plant Physiol. 22*, 167−181.
46. Barter, L. M. C., Bianchietti, M., Jeans, C., Schilstra, M. J., Hankamer, B., Diner, B. A., Barber, J., Durant, J. R., and Klug,

D. R. (2001) Relationship between excitation energy transfer, trapping, and antenna size in photosystem II, *Biochemistry 40*, 4026−4034.
47. Cuni, A., Xiong, L., Sayre, R., Rappaport, F., and Lavergne, J. (2004) Modification of the pheophytin midpoint potential in photosystem II: Modulation of the quantum yield of charge separation and of charge recombination pathways, *Phys. Chem. Chem. Phys. 6*, 4825−4831.
48. Houssier, C., and Sauer, K. (1970) Circular dichroism and magnetic circular dichroism of the chlorophyll and protochlorophyll pigments, *J. Am. Chem. Soc. 92*, 779−791.
49. Katz, J. J., Shipman, L. L., Cotton, T. M., and Janson, T. R. (1978) in *The Porphyrins, Physical Chemistry* (Dolphin, D., Ed.) pp 401, Academic Press: New York.
50. Ivancich, A., Artz, K., Williams, J. C., Allen, J. P., and Mattioli, T. A. (1998) Effects of hydrogen bonds on the redox potential and electronic structure of the bacterial primary electron donor, *Biochemistry 37*, 11812−11820.
51. Lin, X., Murchison, H. A., Nagarajan, V., Parson, W. W., Allen, J. P., and Williams, J. C. (1994) Specific alteration of the oxidation potential of the electron donor in reaction centers from *Rhodobacter sphaeroides*, *Proc. Natl. Acad. Sci. U.S.A. 91*, 10265−10269.
52. Kálmán, L., LoBrutto, R., Allen, J. P., and Williams, J. C. (1999) Modified reaction centers oxidize tyrosine in reactions that mirror photosystem II, *Nature 402*, 696−699.
53. Mimuro, M., Hirayama, K., Uezono, K., Miyashita, H., and Miyachi, S. (2000) Uphill energy transfer in a chlorophyll *d*-dominating oxygenic photosynthetic prokaryote, *Acaryochloris marina*, *Biochim. Biophys. Acta 1456*, 27−34.
54. Hughes, J. L., Prince, B. J., Krausz, E., Smith, P. J., Pace, R. J., and Riesen, H. (2004) Highly efficient spectral hole-burning in oxygen-evolving photosystem II preparations, *J. Phys. Chem. B 108*, 10428−10439.
55. Hughes, J. L., Prince, B. J., Peterson Årsköld, S., Smith, P. J., Pace, R. J., Riesen, H., and Krausz, E. (2004) The native reaction centre of photosystem II: A new paradigm for P_{680}, *Aust. J. Chem. 57*, 1−5.
56. Keren, N., Kidd, M. J., Penner-Hahn, J. E., and Pakrasi, H. B. (2002) A light-dependent mechanism for massive accumulation of manganese in the photosynthetic bacterium *Synechocystis* sp. PCC 6803, *Biochemistry 41*, 15085−15092.

BI048314C